

# Experimental determination of mode II fracture toughness $K_{IIc}$ for joint-grouting material by using electric properties

Q. H. Li

Zhejiang University, Hangzhou, P.R. China

C. X. Yu

Jizhun Fangzhong Architectural Design Associates, Chengdu, P.R. China

S. L. Xu

Zhejiang University, Hangzhou, P.R. China

**ABSTRACT:** An experimental study on mode II fracture of the joint-grouting material between two blocks of the concrete dam is carried out by using the double-edge notched mode II specimens. In consideration of the difficulty in determination of the critical load, the electric property of the joint-grouting material is applied to obtain the critical load of mode II fracture for double-edge notched specimen with preformed joint in the present test. It is found that the  $K_{IIc}$  of the joint-grouting material is dependent on the specimen depth and width, and is independent of initial crack to depth ratio. The experimental results also show that electric resistance increases with the increase of the measured load and displacement, and the behavior of electric resistance of joint-grouting material can be used to determine the critical mode II fracture load which is a basis to ascertain  $K_{IIc}$  values of the joint-grouting material using the double-edge specimen.

## 1 INSTRUCTIONS

During the construction of bulk concrete structures, grouting is always applied between the construction joints to make the structure as a whole to undertake applied load after temperature and deformation of concrete stabilize. However, a relative weak section forms at the joint-grouting interface of dam, where mode II fracture is likely to occur under seismic action or thermal stress. Therefore, the characteristics of the mode II fracture and determination of the corresponding mode II fracture toughness of the grouting construction are very important to guarantee the safe operation of foundational establishment.

In the present work, experiments on mode II fracture of the joint-grouting material, i.e. hardened cement paste, between two blocks of the concrete dam as a model of grouting construction of dam joints have been carried out. Based on the research work of Xu and Reinhardt (Xu et al. 1996, Reinhardt et al. 1997, Reinhardt & Xu 1998, Reinhardt & Xu 2000), the double-edge mode II specimens have been applied. Major test variables include specimen dimensions and ligament length. It is difficult to ascertain the mode II fracture toughness  $K_{IIc}$  due to the determination of the critical mode II cracking load. Therefore, the electric property of the joint-grouting material (Zhang 2006, Sun 2006) has

been applied to monitor mode II fracture process of double-edge specimens in the experiment.

## 2 EXPERIMENTAL STUDY

### 2.1 Double-edge mode II specimens

Figure 1 shows the model of rectangle double-edge notched plate. Middle of the plate is the ligament which stands for grouting joint. The total depth of specimen is  $2h$ , the width is  $2w$ , the ligament length is  $2a$ , and different thicknesses of the plate are used according to the requirement. Mode II fracture toughness  $K_{IIc}$  can be calculated by

$$K_{IIc} = \frac{\sigma}{4} (\pi a)^{1/2} \quad (h \geq 2a \quad \text{and} \quad w \geq \pi a) \quad (1)$$

$$K_{IIc} = \frac{\sigma}{4} w^{1/2} \quad (h \geq 2a \quad \text{and} \quad w \leq \pi a) \quad (2)$$

The condition  $h \geq 2a$  ensures the uniform distribution of stress at the loading end.

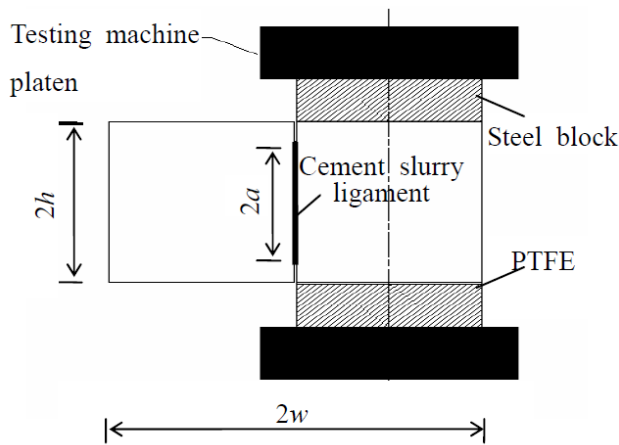


Figure 1. Sketch of the double-edge notched specimen with preformed joint.

## 2.2 Mix proportion and specimen preparation

In this test, P.O.32.5R Portland cement, sand (fineness modulus=2.6, maximum size=1mm), and coarse aggregates (maximum size =10mm) are used. The mix proportion of concrete is  $w:c:s:a = 0.47:1:1.38:3.22$ , and the mix proportion of joint-grouting material is  $w:c = 0.4:1$ . The thickness of grout is 4.5mm. Half of the specimen as Figure 1 shows was molded, and then clamped two parts of specimen after 24 hours. At the same time, two ends of the middle part were spaced by an appropriate sheet. Afterwards the preformed joint was grouted and vibrated slightly. Dimensions of specimens are showed in Table 1 and each group includes six specimens. The influence of width, depth and initial crack to depth ratio on mode II fracture properties of double-edge notched specimen with preformed joint.

During moulding, 10mm×10mm steel meshes were embedded in both sides of specimens, and were 10mm higher than two ends of ligaments (see Fig. 2). After casting, all the specimens were covered with plastic sheets to avoid evaporation and demolded after 24 hours. Then specimens were cured outdoors with water spray once a day.

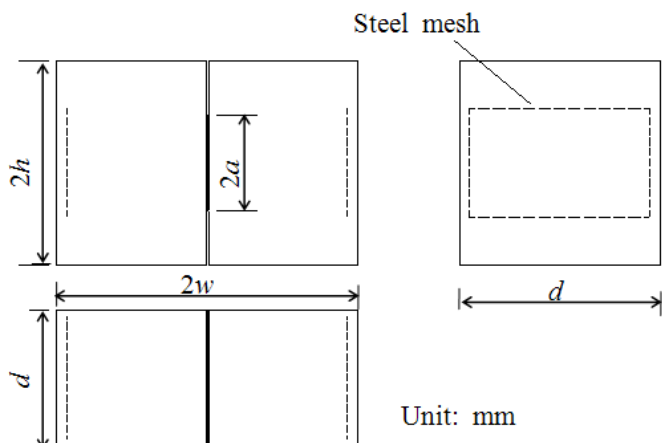


Figure 2. Sketch of steel mesh in specimen.

Table 1. Dimensions of double-edge notched specimens with preformed joint.

width $2w$ (mm)	depth $2h$ (mm)	thickness $d$ (mm)	initial crack length (mm)	initial crack-depth ratio	serial number
200	200	100	20	0.2	A1
			40	0.4	A2
			60	0.6	A3
300	200	100	20	0.2	B1
			40	0.4	B2
			60	0.6	B2
			30	0.2	C1
300	300	100	60	0.4	C2
			90	0.6	C3

## 2.3 Testing procedure

A WKW-3000 testing machine with closed-loop servo-control was used to perform the test. The variation of load, current and displacement was monitored during the experiments under control of load with a constant rate of 80kN/min. To eliminate friction between steel blocks and specimen, a sheet of PTFE was added at bottom and top of specimen. During the testing process, a clip was attached to measure record compressive deformation of loading region in a 150mm gage. To observe crack initiation, electric resistance strain gauges were fixed at the tip of ligament. Resistance measurement device for cementitious composites, voltage sensor and current sensor were used to test resistance of concrete. Impose steady voltage for 10~15 minutes before test to eliminate effect of polarization.

## 3 EXPERIMENTAL RESULTS

### 3.1 Crack pattern of specimens

Typical mode II crack pattern of specimens are shown in Figure 3. It is found that crack propagation along ligament was as follows: when a sudden change occurred in load-displacement relation curve, macroscopic cracks appeared at the tips of ligament; however, the free end of specimen didn't drop. As load increased, cracks propagated continuously till the free end of specimen separated from the loading end, and then the loading end became a compressive column, such as specimens shown in Figure 3 (a) and (b). Sometimes the loading end crushed before the free end of specimen drop (see Fig. 3 (c) and (d)).

It is also found that cracks always generated at the two tips of preformed joint simultaneously and propagated along the ligament till cracks ran-through at the middle of specimen. Because of the shape of preformed joint and the difference between compressive strength of joint-grouting and concrete, cracks may propagated along either left or right side of the grouting.



(a) A2



(b) C3



(c) B2



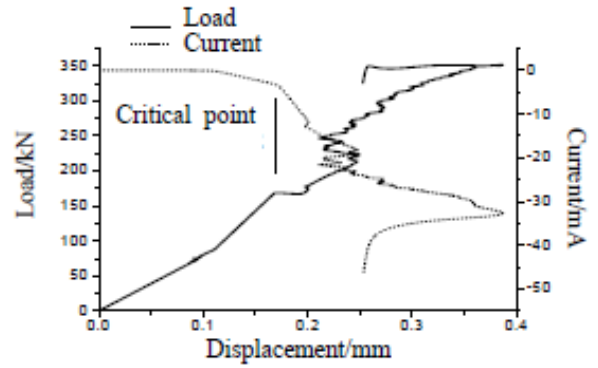
(d) B3

Figure 3. Crack patterns of the specimens.

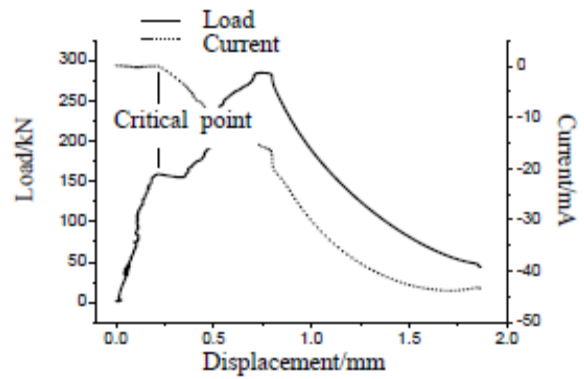
### 3.2 Experimental curves

Figure 4 shows load and current vs. displacement curves of some specimens. Take A1 specimen (see Fig. 4 (a)) as an example, compressive deformation and current present sudden change simultaneously when load reaches 168.53kN. At the moment, cracks

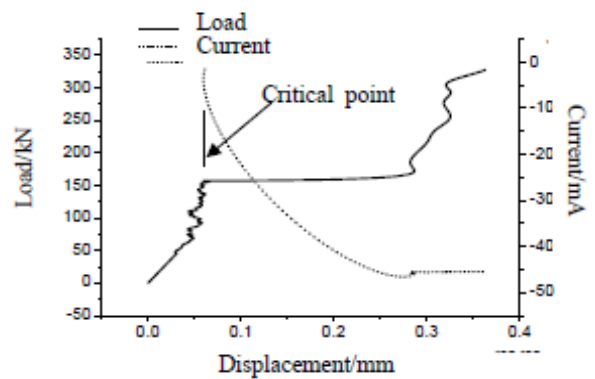
appear at the tips of ligament. With the increase of applied load, cracks propagate along the ligament and finally compressive column crushed. It is a slow process of cracks propagation after first-cracking. That is to say, crack propagation in mode II fracture of joint-grouting also includes crack initiation, stable propagation and final failure, which is similar to mode II fracture process of concrete (Gao et al. 2006).



(a) A1



(b) A2



(c) B2

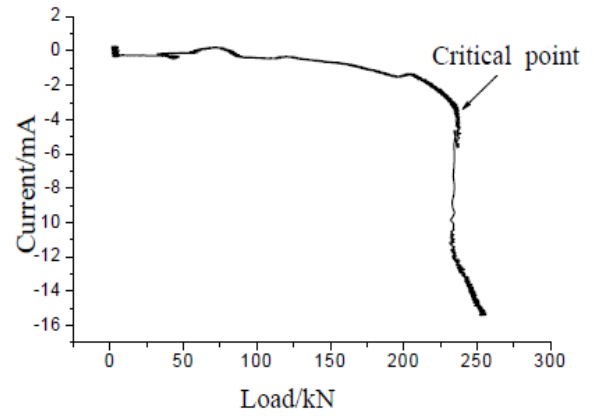
Figure 4. Load and current vs. displacement relation curves.

Compared with load-displacement relation curves, obvious variation can be found in current-displacement relation curves. Current-displacement relation curves of specimens in the present test are quite different from curves in reference (Zhang 2006). No obvious change of current can be found in the beginning. From loading to final failure, three stages

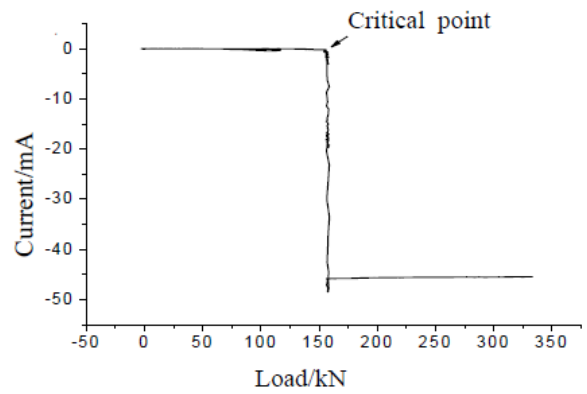
can be divided for current development: little change of current can be found from loading to appearance of mode II cracks; current decreases rapidly as soon as mode II cracks appears; with the increase of applied load, cracks propagate continuously and current still decreases rapidly until final failure. But the decreasing rapid of current in the last stage is slower than the second stage and current drops to the minimum immediately when free end of specimen drops.

Abrupt change points of load- displacement relation curves are always used to determine cracking load (critical load) of mode II fracture together with experimental phenomena. However, it is too difficult to obtain precise value of displacement, especially considering the restraint of outdoor conditions. Therefore, current-load relation curves are used in the test. Take A1 as an example (shown in Fig. 5 (a)), abrupt change of current appears when load reaches 242.11kN, at the same time, cracks occur at the tips of ligament. That is to say, sudden decrease of current is a result of sudden increment of resistance, which is caused by the appearance of cracks. Therefore, the mode II critical load of A1 specimen is equal to 242.11kN. Cracking point of A2 (see Fig. 5 (b)) appears when the current is in descending tendency; therefore, cracks in compressive column come forth earlier than mode II cracks. Cracking point of B2 (see Fig. 5 (c)) is just the turning point of current, which means cracks in compressive column come forth later than mode II cracks. On all accounts, the sequence of these two kinds of cracks varies for different specimens. Moreover, free end of B2 dropped at about 158.5kN, resulting in sudden decrease of current to the minimum (see Fig. 5 (c)).

Figure 6 shows load-CTOD curves of some specimens in the test. Sudden increase of CTOD can be found with the increase of applied load. At that moment, cracks occur at the tips of ligament. Therefore, the critical point can be determined from the change of load-CTOD curves. Similarly to load-CTOD curves, critical point of mode II fracture can also be determined through load - strain of ligament tip relation curves shown in Figure 7.

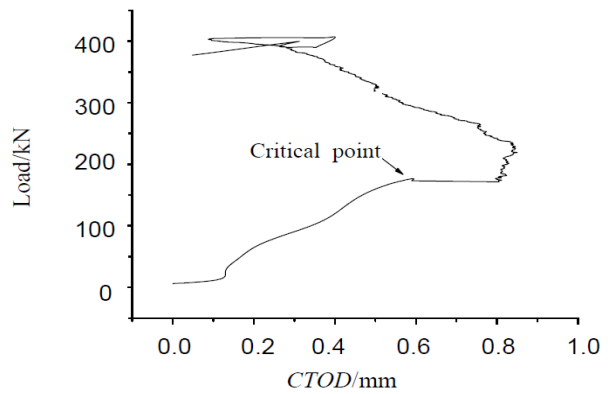


(b) A2

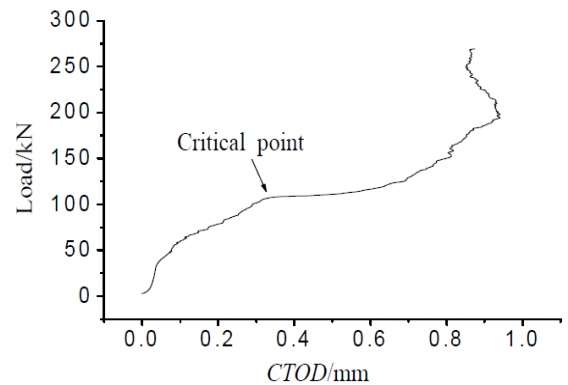


(c) B2

Figure 5. Current-load relation curves.

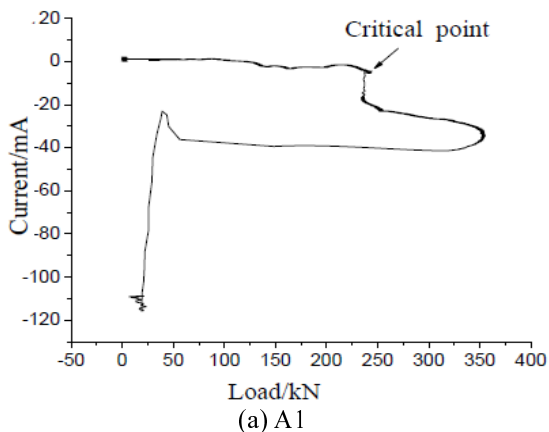


(a) B1

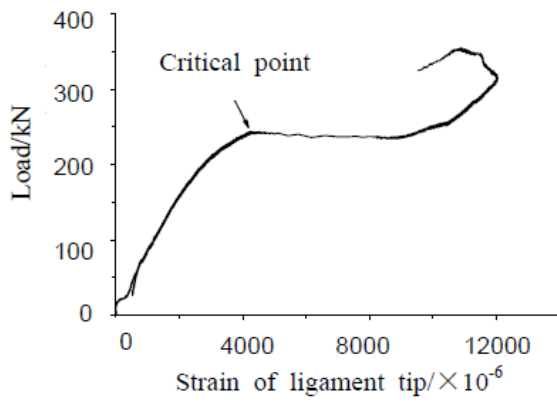


(b) C2

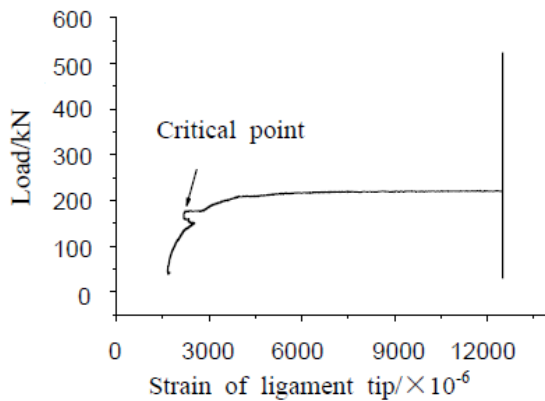
Figure 6. Load-CTOD relation curves.



(a) A1



(a) A1



(b) B2

Figure 7. Load-strain of ligament tip relation curves.

Accordingly, experimental phenomena should be observed to distinguish whether it's mode II fracture or not. And then ascertain critical load  $P_c$  on basis of both experimental phenomena and curves.

### 3.3 Fracture toughness $K_{IIc}$ of joint-grouting material

Formulae (1) and (2) are used to calculate crack tip stress-intensity factor of double-edge notched mode II specimens. After determination of critical load  $P_c$ , fracture toughness  $K_{IIc}$  can be calculated. The calculation is on the basis of the assumption that critical stress  $\sigma_c$  and maximum stress  $\sigma_{max}$  distribute uniformly, so the condition  $h \geq 2a$  could be relaxed. Because the condition  $w \leq \pi a$  is satisfied for all cases, formula (2) can be used to calculate fracture toughness  $K_{IIc}$ . Table 2 shows the testing results.

### 3.4 Influence of depth, width and initial crack-depth ratio on $K_{IIc}$

It can be found in Table 2 that, for different series with the same ligament length,  $K_{IIc}$  declines with the increase of specimen depth ( $K_{IIc}$  of series C is lower than series A and B). Otherwise,  $K_{IIc}$  also presents a decline tendency with the increase of specimen

Table 2. Testing results of joint-grouting specimens.

Specimen	$P_c$ /kN	$P_{max}$ /kN	$P_c / P_{max}$	$\sigma_c$ /MPa	$\sigma_{max}$ /MPa	$K_{IIc}$ /MPam <sup>1/2</sup>
A1-1	186.56	212.3	0.88	18.66	21.23	1.475
A1-2	168.53	351.57	0.48	16.85	35.16	1.332
A1-3	133.99	283.12	0.47	13.4	28.31	1.059
A1-4	124.6			12.46		0.985
A1-5	180.6			18.06		1.428
A1-6	242.11	358.36	0.68	24.21	35.84	1.914
Average				17.27	30.14	1.449
A2-1	236.01	350.78	0.67	23.6	35.08	1.866
A2-2	301.22	376.21	0.8	30.12	37.62	2.381
A2-3	230.09	457.49	0.5	23.01	45.75	1.819
A2-5	236.78			23.68		1.872
A2-6	311.53	449.45	0.69	31.15	44.94	2.463
Average				26.312	40.85	2.08
A3-1	122.83			12.28		0.971
A3-2	116.56			11.65		0.921
A3-3	128.03			12.8		1.012
A3-4	162.89			16.29		1.288
A3-6	127.5			12.75		1.008
Average				13.15		1.04
B1-3	347.11	481.85	0.72	23.14	32.12	2.238*
B1-4	208.77	554.75	0.38	13.92	36.98	1.348
B1-5	221.21	495.16	0.45	14.74	33.01	1.427
B1-6	176.05	406.89	0.43	11.74	27.13	1.138
Average				15.89	32.31	1.304
B2-1	147.71	516.47	0.29	9.85	34.43	0.954
B2-1	356.46	605.34	0.59	23.76	40.36	2.3
B2-3	105.3	495.22	0.21	7.02	33.01	0.68
B2-4	158.5	329.44	0.48	10.57	21.96	1.024
B2-5	294.6	635.69	0.46	19.64	42.38	1.902
B2-6	176.93	522.68	0.34	11.8	34.85	1.143
Average				13.77	34.5	1.334

B3-1	177	408.56	0.43	11.8	27.24	1.143
B3-2	126.38	367.72	0.34	8.43	24.51	0.816
B3-3	355.74	516.47	0.69	23.72	34.45	2.297
B3-4	115.26	269.36	0.43	7.68	17.96	0.744
B3-5	230.96	470.08	0.49	15.4	31.34	1.491
B3-6	196.4	406.89	0.48	13.09	27.13	1.267
Average				13.35	27.11	1.293
C1-1	195.01			13		1.259
C1-2	134.04			8.94		0.866
C1-3	147.3			9.82		0.951
C1-4	156.95			10.46		1.013
C1-5	91.93			6.13		0.594
C1-6	97.47			6.5		0.629
Average				9.14		0.885
C2-2	109.46			7.3		0.707
C2-3	197.78			13.19		1.277
C2-4	139.81			9.32		0.902
C2-5	121.67			8.11		0.785
C2-6	106.63			7.11		0.688
Average				9.01		0.872
C3-1	104.15	511.53		6.94	34.1	0.672
C3-2	102.48			6.83		0.661
C3-3	200.56			13.37		1.295
C3-4	118.89			7.93		0.768
C3-5	126.05			8.4		0.813
C3-6	106.55			7.1		0.687
Average				8.43		0.816

width ( $K_{IIc}$  of series A is lower than series B and C). Depth and width of specimen present obvious size effect on  $K_{IIc}$ , however,  $K_{IIc}$  is almost independent of initial crack-depth ratio.  $K_{IIc}$  of series B and C doesn't show obvious variation with the increase of initial crack-depth ratio ( $K_{IIc}$  of series B is 1.304, 1.334, 1.293, and  $K_{IIc}$  of series C is 0.885, 0.872, 0.816); but the results of series A are discrete, and the possible reason is initial defects of specimens. The conclusion can be drawn that the fracture toughness  $K_{IIc}$  of the joint-grouting material is dependent on the specimen depth and width, and is independent of ligament length.

#### 4 CONCLUSIONS

The electric property of the joint-grouting material has been applied to determine the critical load of mode II fracture for double-edge notched specimen with preformed joint in the present test. The experimental results show that mode II fracture is a gradual propagation process. The mode II crack always initiates either from the interface between grouting material and the compressive block or the interface between grouting material and the free block. By comparison between the relationships of load-displacement, current-displacement, current-load, load-CTOD and load-strain of ligament tip, it has been found that variation of electric resistance of joint-grouting material is obvious and can be used to determine the critical load of mode II fracture, and ascertain  $K_{IIc}$  value of the joint-grouting material using the double-edge notched specimen. A size ef-

fect of specimen dimensions on mode II fracture toughness  $K_{IIc}$  of the joint-grouting material exists. However,  $K_{IIc}$  is independent of initial crack-depth ratio.

#### REFERENCES

- Gao, H.B. Xu, S.L. Wu, Z.M. Bu, D. 2006. Experimental study on fracture toughness  $K_{IIc}$  of concrete. *Journal of Hydroelectric Engineering* 25 (5): 68 - 73. (in Chinese)
- Reinhardt, H.W. & Xu, S.L. 1998. Experimental determination of KIIC of normal strength concrete. *Materials and Structures* 31(209): 296-302.
- Reinhardt, H.W. & Xu, S.L. 2000. A practical testing approach to determine mode II fracture energy GIIF for concrete. *International Journal of Fracture* 105(2): 107-125.
- Reinhardt, H.W. Josko, O. Xu, S.L. & Abebe, D. 1997. Shear of Structural concrete members and pure mode II testing. *Advanced cement based materials* 5 (n3-4): 75-85.
- Sun, J. *Studies on Electric Properties and Applications of Carbon Fiber Reinforced Concrete (CFRC)*. Dalian: Dalian University of Technology, 2006. (in Chinese)
- Xu, S.L. Reinhardt, H.W. & Gappoev, M. 1996. Mode II fracture testing method for highly orthotropic materials like wood. *International Journal of Fracture* 75 (2): 185-214.
- Zhang, D.J. *Studies on Electric Properties of Cementitious Composite Containing Carbon Fibers and Their Applications*. Dalian: Dalin University of Technology, 2006.(in Chinese)